

Hydrogel Formation Using New L-Lysine-Based Low-Molecular-Weight Compounds with Positively Charged Pendant Chains

by Masahiro Suzuki^{*a)}, Mariko Yumoto^{b)}, Mutsumi Kimura^{b)}, Hirofusa Shirai^{b)}, and Kenji Hanabusa^{a)}

^{a)} Graduate School of Science and Technology

^{b)} Department of Functional Polymer Science, Shinshu University, Ueda, Nagano 386-8567, Japan
(fax: 81-268-21-5608; e-mail: msuzuki@giptc.shinshu-u.ac.jp)

Low-molecular-weight compounds based on L-lysine with alkylpyridinium or -imidazolium groups have been synthesized and studied for their gelation behavior in H₂O. Most compounds formed gels below a concentration of 2.5 weight-%, the pyridinium bromide **2a** and the 1-methyl-1*H*-imidazolium bromide **3** even at 0.1 weight-%. The minimum gel concentration (MGC) necessary for hydrogelation increased with increasing length of the Lys *N*^α-alkanoyl chain, but the gelation ability concomitantly decreased. Electron-microscopic images demonstrated that these hydrogelators create a three-dimensional network in H₂O by entanglement of self-assembled nanofibers. A fluorescence study with 8-anilinonaphthalene-1-sulfonic acid (ANS) proved that some hydrophobic aggregates are formed at hydrogelator concentrations below an MGC of less than 50 μM (0.004%). FT-IR, ¹H-NMR, and Fluorescence studies indicated that the driving forces for the self-assembly into nanofibers are mainly hydrophobic interactions and H-bonding between amide groups.

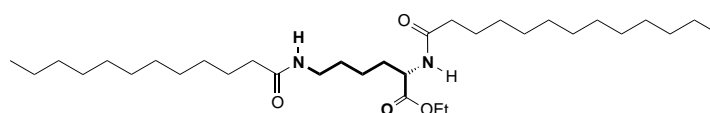
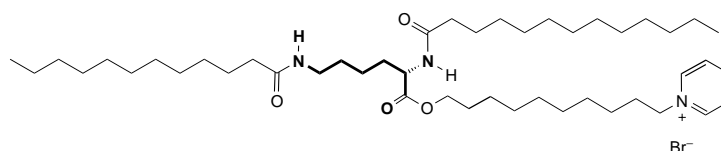
Introduction. – Organogels, in which organic solvents are gelled by low-molecular-weight compounds (organogelators), have attracted much interest due to their unique features and potential applications as organic soft materials [1]. Many organogelators have been reported in the literature [2]. Organogelators organize monomeric species into complex higher-ordered structures such as fibrous, tubular, and helical assemblies in organic solvents by means of H-bonding, π/π -stacking, *Van der Waals*, and charge-transfer interactions. Such nanostructures create three-dimensional networks by the entanglements of nanofibers, which lead to the gelation of organic solvents. Furthermore, organogels have been used for the fabrication of templated materials [3], sensors [4], and assemblies with molecular-recognition and other properties [5].

Hydrogels have been extensively investigated because of their potential applications for superabsorption, drug-delivery materials, and tissue-engineering scaffolds, as well as for the development of new materials that reversibly respond to various external stimuli [6][7]. They have been traditionally constructed with hydrophilic high-molecular-weight polymers, physically or chemically cross-linked, containing a large amount of H₂O in the interstitial spaces. In such hydrogels, complicated intermolecular association modes are found. Classical gels formed by entanglement and cross-linking of linear high-molecular-weight polymers exhibit similar morphological properties, and there is no controllable ordering or discernible nano- and microstructure beyond local intermolecular associations on a molecular level.

Recently, the construction of hydrogels *via* self-assembly of low-molecular-weight compounds (hydrogelators) has been explored [8][9]. Such hydrogelators give rise to nanostructures (fibers, ribbons, tapes, sheets, *etc.*) and then produce gel networks with

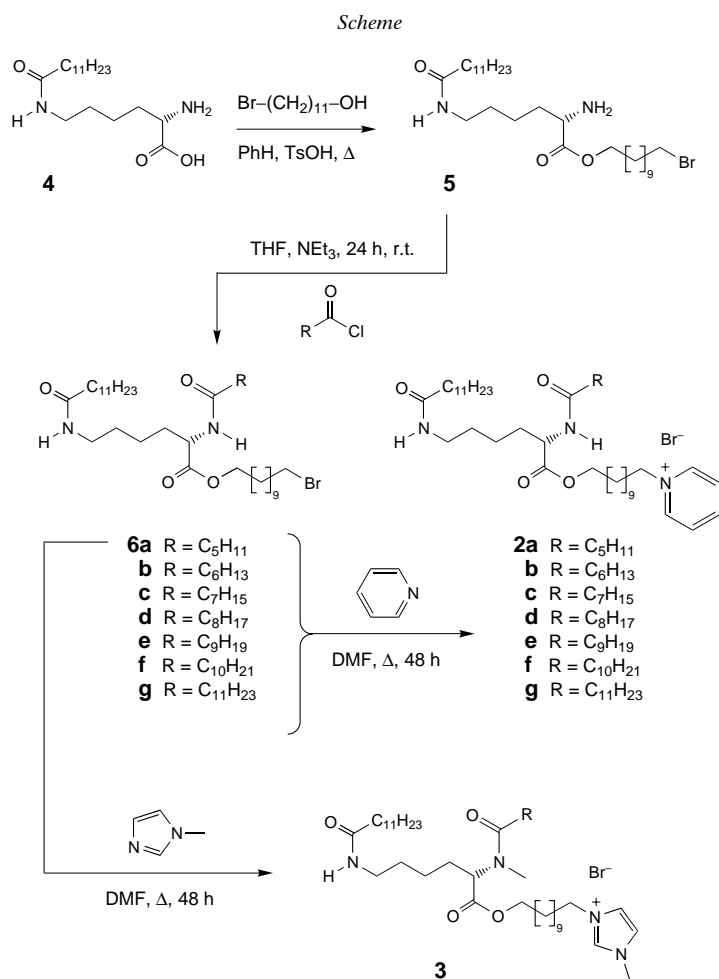
tunable properties, just like organogelators in organic solvents. Using the self-assembling tendency of organogelators, we have attempted to develop organogelators as hydrogelators. To function as hydrogelators, the compounds must be water-soluble. However, most of the known organogelators are difficult to dissolve in H₂O because they incorporate both hydrophilic segments (such as amides, ureas, COOH, and OH groups) and hydrophobic parts (alkyl, nitro, and aromatic groups). A common strategy to solve this problem is the introduction of a permanent charge.

We have developed the L-lysine-based organogelator/hydrogelator **1** by the introduction of a terminal pyridinium group [9]. Compound **1** is an excellent hydrogelator that can gel H₂O at a concentration of 0.2 weight-%. Here, we describe the synthesis and properties of new hydrogelators based on L-lysine containing a positively charged pendant chain.

L-Lysine-based *organogelator*L-Lysine-based *hydrogelator 1* [9]

Results and Discussion. – *Synthesis of Hydrogelators.* Compounds **2a–g** and **3** could be readily prepared from commercially available *N*^ε-lauroyl-L-lysine (**4**) according to the *Scheme*. The Lys COOH group was esterified with 11-bromoundecan-1-ol, and the resulting product **5** was *N*^α-acylated with hexanoyl chloride to afford **6a**. The latter was converted to **2a** and **3** by substitution with either pyridine or 1-methyl-1*H*-imidazole, respectively. Compounds **2b–g** were prepared analogously from the corresponding acylated precursors **6b–g**.

Gelation Tests. – The results of the gelation test and the values of the minimum gelation concentration (MGC) necessary for hydrogel formation with compounds **1–3** are listed in *Table 1*. Except for the highly water-soluble **2f**, all compounds displayed excellent gelation abilities in H₂O. In particular, **2a** and **3** formed *transparent* hydrogels at 0.1 weight-% concentration. These hydrogels are very stable and maintain the gel state for at least 6 months. Very interestingly, the MGC values significantly depend on the length of the Lys *N*^α-alkanoyl chain, and the gelation ability decreases with increasing chain length. Furthermore, the hydrogels become opaque with increasing length of the alkanoyl chain, probably due to an increase in the size of the nanostructure.

Table 1. Gelation Properties of **1**–**3** in H₂O. The data for **1** have been taken from [9].

	1	2a	2b	2c	2d	2e	2f	2g	3
MGC ^{a)}	3	1	3	10	13	15	^{d)}	25	1
Appearance ^{b)}	T	T	TL	O	O	O	S	O	T
N _{H₂O} ^{c)}	12,500	41,000	14,000	4,300	3,300	2,900	–	1,800	41,000

^{a)} Minimum gel concentration for gelation, in mg/ml (accuracy: ± 0.5). ^{b)} T = transparent, TL = translucent, O = opaque, S = solution at 3 weight-%. ^{c)} Number of H₂O molecules entrapped per gelator molecule.

Microscopic Studies. Fig. 1 shows the TEM and FE-SEM¹⁾ images to samples prepared from **2a** and **3** in H₂O. In the hydrogels, these hydrogelators create a three-

¹⁾ TEM and FE-SEM stand for transmission and field-emission scanning electron microscopy, respectively.

dimensional network formed by entanglement of the *fine* fibers (diameters of *ca.* 20–40 nm). Therefore, initial formation of the hydrogels is caused by entrapping water (solvent) molecules in the spaces of the network, like in common organogels. The TEM images of these hydrogels demonstrated that there are larger fibers (*ca.* 50–70 nm in diameter) in the case of **2a**, **2b**, and **3**, and even larger ones (100–200 nm) for **2c–2g** (except for **2f**). We have reported that the properties of the hydrogels significantly depend on the diameter of the self-assembled fibers [9]. In the present case, the hydrogels formed by the fine fibers (*ca.* 20–40 nm) and the relatively bold fibers (*ca.* 100–200 nm) appear transparent and opaque, respectively, whereas nanofibers with an intermediate diameter (*ca.* 50–70 nm) create translucent materials. This can be explained most likely by differential intermolecular interactions that are stronger in the cases of the compounds with longer alkanoyl chains, leading to larger nanofibers.

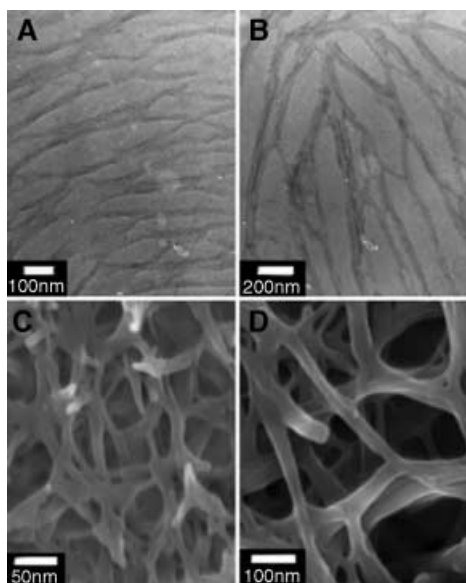


Fig. 1. TEM and FE-SEM Images of samples prepared from **2a** (A, C) and **3** (B, D) in H_2O

Fluorescence Studies. To evaluate the self-assembly behavior, we recorded the fluorescence spectra of 8-anilino-naphthalene-1-sulfonic acid (ANS) in an aqueous solution of **2a**. ANS is a fluorescent probe sensitive to changes in hydrophobic environments. Fig. 2 shows the dependence of the luminescence maxima (λ_{max}) and fluorescence intensities I_0 and I at λ_{max} in the absence and in the presence of **2a**, respectively. Very interestingly, the bathochromic shifts from 530 to 461 nm and the luminescence intensity both decrease with increasing concentration of **2a** up to $50 \mu M$, which is much lower than the corresponding MGC. A similar blue-shift is observed when ANS is transferred from bulk H_2O into more hydrophobic environments. Apparently, **2a** forms some kind of aggregates below its MGC. The observed fluorescence quenching is then induced by ‘concentration’ of the ANS molecules within the hydrophobic aggregate domains.

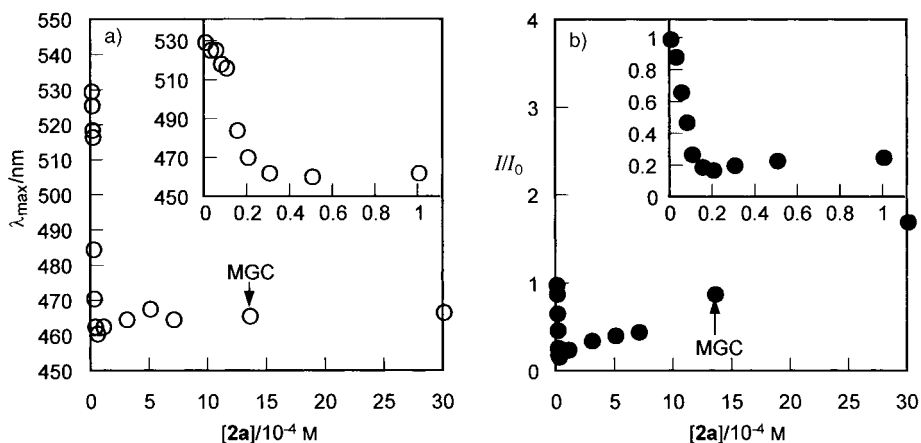


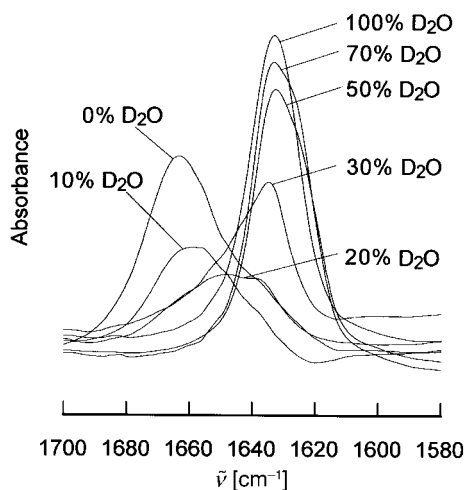
Fig. 2. Luminescence maxima (a) and rel. luminescence intensities (b) of ANS as a function of **2a**. [ANS] = 1.0×10^{-5} M. Inset: the low-concentration range.

Further addition of **2a** increases the luminescence intensity of ANS, but induces only a slight change in λ_{max} . This indicates that the interior of the strands in the self-assembled nanofibers has almost the same hydrophobicity as that of the aggregates formed at lower concentration. Also, the dispersion of ANS molecules restricts the quenching, leading to an increase in fluorescence intensity. Our results, thus, suggest a hydrophobic driving force for the self-assembly of **2a** into nanofibers, which is in agreement with previous findings [9].

Apparently, the self-assembly of **2a** proceeds in two steps: up to a concentration of $50 \mu\text{M}$, the molecules are aggregated (sharp blue-shift and decrease in I/I_0), before they self-assemble into nanofibers (very slight red-shift and increase in I/I_0).

FT-IR Study. It is well-known that H-bonding is one of the driving forces for the self-assembly of organogelators in organic solvents [1][2]. Although *Fourier-transform infrared* (FT-IR) spectroscopy is a powerful tool to study such interactions, it is very difficult to obtain meaningful information in H_2O . Thus, the FT-IR spectra of **2a** were measured in $\text{D}_2\text{O}/(\text{D}_6)\text{DMSO}$ mixtures (Fig. 3), and the results are listed in Table 2. The IR spectrum in neat $(\text{D}_6)\text{DMSO}$ showed absorption bands at 1663 and 1546 cm^{-1} , characteristic of non-H-bonded C=O (amide I) stretching and H-bonded N–H (amide II) bending vibrations, respectively. In CHCl_3 , these resonances appeared at 1660 and 1515 cm^{-1} , respectively. Since CHCl_3 does neither interact with hydrogelators nor induces their self-assembly, the amide N–H groups in **2a** interact only with DMSO [$(\text{CD}_3)_2\text{S}=\text{O} \cdots \text{H}-\text{N}$], and the amide C=O groups are not involved. With increasing D_2O content, the bands of the amide-I resonances are dramatically shifted from 1663 to 1633 cm^{-1} (threshold value for D_2O content $\geq 50\%$). In contrast, the absorbance decreases up to a 20% D_2O content, and then it increases. Such spectral shifts are compatible with the presence of intermolecularly H-bonded amide groups, which suggests that H-bonding is a major driving force for hydrogel formation.

The above IR data also provide information on the alkyl groups. The absorption bands of the asymmetric (ν_{as}) and symmetric (ν_{s}) CH_2 stretching vibrations of **2a**

Fig. 3. FT-IR Spectra of **2a** in (D_6)DMSO/ D_2O mixtures

appeared at 2926 (ν_{as}) and 2856 cm^{-1} (ν_s) in (D_6)DMSO, and at 2929 and 2856 cm^{-1} in CHCl_3 , respectively. However, in D_2O , they were shifted to 2916 and 2848 cm^{-1} . It is well-known that these IR bands are shifted to lower frequencies when the flexibility of the alkyl chains is decreased [10]. Considering this, the alkyl groups of **2a** must be strongly restricted in D_2O due to self-assembly by means of hydrophobic interactions.

Table 2. FT-IR Data of **2a** in (D_6)DMSO/ D_2O Mixtures and in CHCl_3

D_2O [%]	ν (C=O) (ester)	ν (C=O) (amide I)	δ (N-H) (amide II)	ν_{as} (C-H)	ν_s (C-H)
0	1736	1663	1546	2926	2856
10	1735	1657	a)	2909 (sh)	2856
20	1735	1648, 1637	a)	2910 (sh)	2856
30	1736	1635	a)	2913 (sh)	2856
50	1737	1633	a)	2915	2848
70	1737	1633	a)	2915	2848
100	1739	1633	a)	2916	2848
CHCl_3	1741	1658	1513	2929	2856

a) Not detected because of H/D exchange.

¹H-NMR Study. To obtain further information on intermolecular H-bonding interactions between amide groups, we recorded ¹H-NMR spectra of **2a**. Since amide H-atoms do not appear in ¹H-NMR spectra recorded in D_2O , experiments were carried out in (D_6)DMSO/ H_2O mixtures²⁾ (Fig. 4 and Table 3). With increasing H_2O content, the amide resonances were shifted to lower field (up to 20% H_2O), and then shift upfield, (>20% H_2O), indicating different types of H-bonding: $(\text{CD}_3)_2\text{SO} \cdots \text{H-N}$ vs. $\text{H}_2\text{O} \cdots \text{H-N}$ [11]. Furthermore, the upfield shifts of the amide NH signal at H_2O

²⁾ The maximum H_2O content was 50%. Higher concentrations led to solutions too viscous to provide meaningful ¹H-NMR data.

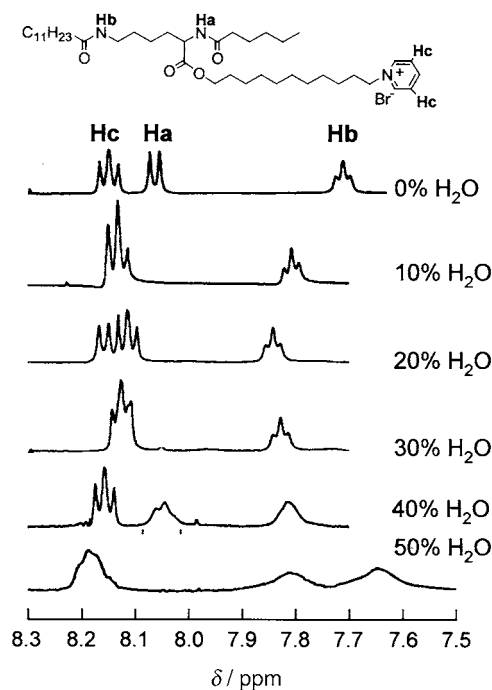


Fig. 4. $^1\text{H-NMR}$ Spectra of **2a** in $(D_6)\text{DMSO}/\text{H}_2\text{O}$ mixtures

concentrations above 20% indicate intermolecular H-bonding between amide groups, which agrees with the results obtained by IR spectroscopy.

Interestingly, the pyridinium H_c signals were shifted upfield up to a content of 20% H_2O , and then to lower field. This shift might be explained by solvation effects. The addition of H_2O brings about the hydration of the charged pyridinium rings, which would lead to the observed upfield shift. Further addition of H_2O then induces **2a** to self-assemble, probably under release of H_2O , which, in turn, would explain the shift of the pyridinium H_c signals to lower field.

Table 3. $^1\text{H-NMR}$ Chemical Shifts of Amide Resonances of **2a** in $(D_6)\text{DMSO}/\text{H}_2\text{O}$ Mixtures

H_2O [%]	$\delta(\text{N-H}_a)$	$\delta(\text{N-H}_b)$
0	8.07	7.72
10	^{a)}	7.80
20	8.16	7.84
30	^{a)}	7.82
40	8.05	7.81
50	7.81	7.65

^{a)} Not visible (overlapping with arom. H).

Conclusions. – Several new members of charged L-lysine-based low-molecular-weight hydrogelators, especially **2a**, **2b**, and **3**, are excellent hydrogelators. Compounds

2a and **3** can gel H₂O at 0.1 weight-%, corresponding to entrapping more than 40,000 H₂O molecules per gelator molecule. TEM Observations of the hydrogels demonstrate the creation of three-dimensional networks formed by entangled, self-assembled nanofibers. FT-IR ¹H-NMR, and Fluorescence measurements indicate that these compounds first self-assemble into aggregates containing hydrophobic sites at very low hydrogelator concentration, and then grow into nanofibers with increasing concentration, mainly *via* hydrophobic and H-bonding interactions.

This study was supported by a Grant (No. 1465358) and a Grant-in-Aid for Scientific Research on Priority Areas (A) (No. 413/13031036) from the *Ministry of Education, Sports, Culture, Science, and Technology of Japan*, and *The Kao Foundation for Arts and Science*, respectively.

Experimental Part

General. *N*^ε-Lauroyl-L-lysine was obtained from *Ajinomoto Co., Inc.* All other chemicals were of the highest grade commercially available and used without further purification. All solvents used in the syntheses were purified, dried, or freshly distilled. Gelation tests were carried out as follows: a mixture of a weighed gelator in H₂O (1 ml) in a sealed test tube was heated at *ca.* 40° until a clear soln. appeared. After allowing the solns. to stand at 25° for 6 h, their state was evaluated by the so-called 'stable-to-inversion-of-a-test-tube' method reported by *Hanabusa et al.* [5]. Fluorescence spectra were recorded on a *JASCO FP-750* spectrofluorometer at a conc. of 10⁻⁵ M ANS and 0–10 mm gelator; the excitation wavelength was 365 nm (absorption maximum). FT-IR Spectra were recorded on a *JASCO FS-420* spectrometer in CHCl₃ (15 mg ml⁻¹ of gelator) and in (D₆)DMSO/D₂O (20 mg ml⁻¹ of gelator) operating at a 2-cm⁻¹ resolution with 32 scans and using a cell with a CaF₂ window, and 25-μm spacers in DMSO/D₂O or 200-μm spacers in CHCl₃. ¹H-NMR Spectra were recorded on a *Bruker AVANCE-400* spectrometer with TMS as internal standard; solns. of **2a** (20 mg ml⁻¹) were prepared in (D₆)DMSO/H₂O mixtures. Elemental analyses were performed on a *Perkin-Elmer Series II CHNS/O Analyzer 2400*. TEM Images were obtained using a *JEOL JEM-2010* electron microscope at 200 kV. Samples were prepared as follows: the aq. solns. of the gelators were dropped on a collodion- and carbon-coated 400-mesh copper grid and immediately dried *in vacuo* for 24 h. After dropping a phosphotungstic acid soln. (2 weight-%), the grids were dried under reduced pressure for 24 h. SEM Images were obtained using a *Hitachi S-5000* field-emission scanning electron microscope. Samples for FE-SEM measurements were dried overnight *in vacuo* before observation. The dried samples were sputtered using a gold target.

N^ε-Lauroyl-L-lysine 11-Bromoundecyl Ester (**5**). A benzene soln. (400 ml) of *N*^ε-lauroyl-L-lysine (**4**; 60 mmol), 11-bromoundecan-1-ol (50 mmol), and toluenesulfonic acid (TsOH) monohydrate (130 mmol) was heated at 130° for 48 h using a *Dean–Stark* trap. The excess benzene was evaporated, the residue was dissolved in MeOH (100 ml), and morpholine (200 mmol) was added with stirring. The white precipitate was filtered off, and the filtrate was concentrated to *ca.* 50 ml. The soln. was added to a large excess of H₂O (2 l) with vigorous stirring. The white precipitate was filtered, washed with H₂O, and dried. The crude product was recrystallized twice from MeOH/Et₂O to afford 80% of **5**. M.p. 58–60°. IR (KBr): 3451, 3332, 1736, 1642, 1532. ¹H-NMR (400 MHz, CDCl₃): 0.88 (*t*, *J* = 6.6, Me); 2.14 (*t*, *J* = 7.8, Hz, CH₂CONH); 3.24 (*q*, *J* = 6.0, NHCH₂); 6.42–3.45 (*m*, CH). Anal. calc. for C₂₂H₅₇BrN₂O₃ (561.68): C 62.01, H 10.23, N 4.99; found: C 62.34, H 10.51, N 5.03.

N^ε-Hexanoyl-*N*^ε-lauroyl-L-lysine 11-Bromoundecyl Ester (**6a**). To an anh. THF soln. (400 ml) of **5** (20 mmol) and NEt₃ (10 ml), hexanoyl chloride (24 mmol) was added with stirring. After 24 h at r.t., the white precipitate was hot-filtered, and the filtrate was evaporated to dryness. The product was recrystallized twice AcOEt/MeOH to afford 94% of **6a**. M.p. 72–74°. IR (KBr): 3310, 1734, 1639, 1543. ¹H-NMR (400 MHz, CDCl₃): 0.88–0.90 (*m*, 2 Me); 2.15 (*t*, *J* = 7.3, CH₂CONH); 2.23 (*t*, *J* = 7.0, NHCOCH₂); 3.23 (*q*, *J* = 6.6, NHCH₂); 3.75 (*t*, *J* = 4.6, CH₂Br); 4.12 (*t*, *J* = 6.6, OCH₂); 4.56 (*m*, CHNH); 5.72 (*t*, *J* = 5.3, N^εH); 6.18 (*d*, *J* = 7.8, N^εH). Anal. calc. for C₃₃H₆₇BrN₂O₄ (659.82): C 63.71, H 10.23, N 4.25; found: C 63.99, H 10.55, N 4.37.

N^ε-Heptanoyl-*N*^ε-lauroyl-L-lysine 11-Bromoundecyl Ester (**6b**). Same procedure as for **6a**, but with heptanoyl chloride. Yield: 94%. M.p. 73–75°. IR (KBr): 3311, 1723, 1639, 1543. ¹H-NMR (400 MHz, CDCl₃): 0.86–0.89 (*m*, 2 Me); 2.15 (*t*, *J* = 7.3, CH₂CONH); 2.23 (*t*, *J* = 7.0, NHCOCH₂); 3.23 (*q*, *J* = 6.6, NHCH₂); 3.74 (*t*, *J* = 4.8, CH₂Br); 4.12 (*t*, *J* = 6.8, OCH₂); 4.54–4.59 (*m*, CHNH); 5.75 (*t*, *J* = 5.3, N^εH); 6.20 (*d*, *J* = 7.8, N^εH). Anal. calc. for C₃₆H₆₉BrN₂O₄ (673.35): C 64.17, H 10.32, N 4.16; found: C 64.22, H 10.45, N 4.22.

N^α-Octanoyl-*N*^ε-lauroyl-L-lysine 11-Bromoundecyl Ester (**6c**). Same procedure as for **6a**, but with octanoyl chloride. Yield: 96%. M.p. 75–76°. IR (KBr): 3312, 1727, 1639, 1543. ¹H-NMR (400 MHz, CDCl₃): 0.86–0.89 (*m*, 2 Me); 2.15 (*t*, *J* = 7.6, CH₂CONH); 2.23 (*t*, *J* = 7.8, NHCOCH₂); 3.23 (*q*, *J* = 6.3, NHCH₂); 3.74 (*t*, *J* = 4.8, CH₂Br); 4.12 (*t*, *J* = 6.8, OCH₂); 4.54–4.59 (*m*, CHNH); 5.7 (*t*, *J* = 5.3, N^αHCO); 6.16 (*d*, *J* = 7.8, N^εH). Anal. calc. for C₄₂H₇₆BrN₃O₄ (766.97): C 65.77, H 9.99, N 5.48; found: C 65.89, H 10.20, N 5.54.

N^α-Nonanoyl-*N*^ε-lauroyl-L-lysine 11-Bromoundecyl Ester (**6d**). Same procedure as for **6a**, but with nonanoyl chloride. Yield: 91%. M.p. 82–83°. IR (KBr): 3313, 1727, 1639, 1543. ¹H-NMR (400 MHz, CDCl₃): 0.88–0.90 (*m*, 2 Me); 2.15 (*t*, *J* = 7.3, CH₂CONH); 2.23 (*t*, *J* = 7.0, NHCOCH₂); 3.23 (*q*, *J* = 6.6, NHCH₂); 3.75 (*t*, *J* = 4.6, CH₂Br); 4.12 (*t*, *J* = 6.6, OCH₂); 4.53–4.58 (*m*, CHNH); 5.71 (*t*, *J* = 5.3, N^αH); 6.15 (*d*, *J* = 7.8, N^εH). Anal. calc. for C₃₈H₇₃BrN₂O₄ (701.90): C 65.02, H 10.48, N 3.99; found: C 65.19, H 10.86, N 4.06.

N^α-Decanoyl-*N*^ε-lauroyl-L-lysine 11-Bromoundecyl Ester (**6e**). Same procedure as for **6a**, but with decanoyl chloride. Yield: 96%. M.p. 87–88°. IR (KBr): 3311, 1724, 1638, 1544. ¹H-NMR (400 MHz, CDCl₃): 0.86–0.89 (*m*, 2 Me); 2.15 (*t*, *J* = 7.3, CH₂CONH); 2.23 (*t*, *J* = 7.1, NHCOCH₂); 3.24 (*q*, *J* = 5.8, NHCH₂); 3.76 (*t*, *J* = 4.5, CH₂Br); 4.12 (*t*, *J* = 6.8, OCH₂); 4.53–4.58 (*m*, CHNH); 5.75 (*t*, *J* = 5.3, N^αHCO); 6.20 (*d*, *J* = 7.8, N^εH). Anal. calc. for C₃₉H₇₅BrN₂O₄ (715.93): C 65.43, H 10.56, N 3.91; found: C 65.55, H 10.86, N 3.99.

N^α-Undecanoyl-*N*^ε-lauroyl-L-lysine 11-Bromoundecyl Ester (**6f**). Same procedure as for **6a**, but with undecanoyl chloride. Yield: 96%. M.p. 87–88°. IR (KBr): 3314, 1720, 1636, 1543. ¹H-NMR (400 MHz, CDCl₃): 0.88 (*t*, *J* = 6.6, 2 Me); 2.15 (*t*, *J* = 7.3, CH₂CONH); 2.23 (*t*, *J* = 6.8, NHCOCH₂); 3.23 (*q*, *J* = 6.6, NHCH₂); 3.76 (*t*, *J* = 4.8, CH₂Br); 4.12 (*t*, *J* = 6.8, OCH₂); 4.53–4.58 (*m*, CHNH); 5.71 (*t*, *J* = 5.3, N^αH); 6.17 (*d*, *J* = 7.8, N^εH). Anal. calc. for C₄₀H₇₇BrN₂O₄ (729.95): C 65.82, H 10.63, N 3.84; found: C 66.00, H 11.06, N 3.84.

N^α-Dodecanoyl-*N*^ε-lauroyl-L-lysine 11-Bromoundecyl Ester (**6g**). Same procedure as for **6a**, but with heptanoyl chloride. Yield: 96%. M.p. 90–92°. IR (KBr): 3314, 1725, 1637, 1543. ¹H-NMR (400 MHz, CDCl₃): 0.88 (*t*, *J* = 6.6, Me); 2.15 (*t*, *J* = 7.3, CH₂CONH); 2.23 (*t*, *J* = 7.0, NHCOCH₂); 3.23 (*q*, *J* = 6.3, NHCH₂); 3.74 (*t*, *J* = 4.6, CH₂Br); 4.12 (*t*, *J* = 6.6, OCH₂); 4.56 (*m*, CHNH); 5.64 (*br.*, N^αH); 6.13 (*d*, *J* = 7.8, N^εH). Anal. calc. for C₄₁H₇₉BrN₂O₄ (743.98): C 66.19, H 10.70, N 3.77; found: C 66.33, H 11.16, N 3.79.

1-[(2*S*)-6-[Dodecanoyl(amino)]-2-[hexanoyl(amino)]hexanoyloxy]undecylpyridinium Bromide (**2a**). A DMF soln. (20 ml) of **6a** (10 mmol) and pyridine (100 mmol) was heated at 100° for 48 h under N₂. Et₂O (150 ml) was added, and the soln. was allowed to stand in a refrigerator for 6 h. The white precipitate was filtered, washed with Et₂O, dried, and recrystallized from AcOEt/MeOH to afford 92% of **2a**. M.p. 78–79°. IR (KBr): 3310, 1730, 1639, 1544. ¹H-NMR (400 MHz, CDCl₃): 0.88–0.90 (*m*, 2 Me); 2.17 (*t*, *J* = 8.1, CH₂CONH); 2.25 (*t*, *J* = 7.3, NHCOCH₂); 3.22 (*q*, *J* = 3.9, NHCH₂); 4.05–4.16 (*m*, OCH₂); 4.49 (*m*, CHNH); 6.25 (*t*, *J* = 5.6, N^αH); 6.58 (*d*, *J* = 7.6, N^εH); 8.15 (*t*, *J* = 6.8, 2 arom. H); 8.52 (*t*, *J* = 7.6, arom. H); 9.50 (*t*, *J* = 5.3, 2 arom. H). Anal. calc. for C₄₀H₇₂BrN₃O₄ (738.92): C 65.02, H 9.82, N 5.69; found: C 65.34, H 10.11, N 5.74.

1-[(2*S*)-6-[Dodecanoyl(amino)]-2-[heptanoyl(amino)]hexanoyloxy]undecylpyridinium Bromide (**2b**). Same procedure as for **2a**, but with **6b**. Yield: 92%. M.p. 82–83°. IR (KBr): 3310, 1727, 1638, 1544. ¹H-NMR (400 MHz, CDCl₃): 0.86–0.90 (*m*, 2 Me); 2.18 (*t*, *J* = 8.1, CH₂CONH); 2.27 (*t*, *J* = 7.3, NHCOCH₂); 3.22 (*q*, *J* = 3.9, NHCH₂); 4.05–4.16 (*m*, OCH₂); 4.46–4.49 (*m*, CHNH); 6.24 (*t*, *J* = 5.6, N^αH); 6.59 (*d*, *J* = 7.6, N^εH); 8.12 (*t*, *J* = 6.8, 2 arom. H); 8.55 (*t*, *J* = 7.6, arom. H); 9.51 (*t*, *J* = 5.3, 2 arom. H). Anal. calc. for C₄₁H₇₄BrN₃O₄ (752.95): C 65.40, H 9.91, N 5.58; found: C 65.59, H 10.21, N 5.64.

1-[(2*S*)-6-[Dodecanoyl(amino)]-2-[octanoyl(amino)]hexanoyloxy]undecylpyridinium Bromide (**2c**). Same procedure as for **2a**, but with **6c**. Yield: 91%. M.p. 82–83°. IR (KBr): 3312, 1727, 1639, 1543. ¹H-NMR (400 MHz, CDCl₃): 0.88–0.90 (*m*, 2 Me); 2.17 (*t*, *J* = 8.1, CH₂CONH); 2.25 (*t*, *J* = 7.3, NHCOCH₂); 3.22 (*q*, *J* = 3.9, NHCH₂); 4.06–4.16 (*m*, OCH₂); 4.49–5.04 (*m*, CHNH); 6.26 (*t*, *J* = 5.6, N^αH); 6.59 (*d*, *J* = 7.6, N^εH); 8.15 (*t*, *J* = 6.8, 2 arom. H); 8.52 (*t*, *J* = 7.6, arom. H); 9.51 (*t*, *J* = 5.3, 2 arom. H). Anal. calc. for C₄₂H₇₆BrN₃O₄ (766.97): C 65.77, H 9.99, N 5.48; found: C 65.89, H 10.20, N 5.54.

1-[(2*S*)-6-[Dodecanoyl(amino)]-2-[nonanoyl(amino)]hexanoyloxy]undecylpyridinium Bromide (**2d**). Same procedure as for **2a**, but with **6d**. Yield: 90%. M.p. 83–84°. IR (KBr): 3313, 1727, 1639, 1543. ¹H-NMR (400 MHz, CDCl₃): 0.88–0.90 (*m*, 2 Me); 2.17 (*t*, *J* = 8.1, CH₂CONH); 2.25 (*t*, *J* = 7.3, NHCOCH₂); 3.22 (*q*, *J* = 3.9, NHCH₂); 4.05–4.16 (*m*, OCH₂); 4.47–5.01 (*m*, CHNH); 6.25 (*t*, *J* = 5.6, N^αH); 6.56 (*d*, *J* = 7.6, N^εH); 8.15 (*t*, *J* = 6.8, 2 arom. H); 8.52 (*t*, *J* = 7.6, arom. H); 9.48 (*t*, *J* = 5.3, 2 arom. H). Anal. calc. for C₄₃H₇₈BrN₃O₄ (781.00): C 66.13, H 10.07, N 5.38; found: C 66.24, H 10.28, N 5.44.

1-[(2*S*)-2-[Decanoyl(amino)]-6-[dodecanoyl(amino)]hexanoyloxy]undecylpyridinium Bromide (**2e**). Same procedure as for **2a**, but with **6e**. Yield: 97%. M.p. 88–89°. IR (KBr): 3307, 1738, 1638, 1545. ¹H-NMR (400 MHz, CDCl₃): 0.88–0.90 (*m*, 2 Me); 2.17 (*t*, *J* = 8.1, CH₂CONH); 2.23 (*t*, *J* = 7.3, NHCOCH₂); 3.22 (*q*, *J* = 3.9, NHCH₂); 4.05–4.16 (*m*, OCH₂); 4.49–5.04 (*m*, CHNH); 6.25 (*t*, *J* = 5.6, N^αH); 6.58 (*d*, *J* = 7.6, N^εH); 8.19

(*t*, *J* = 6.8, 2 arom. H); 8.55 (*t*, *J* = 7.6, arom. H); 9.50 (*t*, *J* = 5.3, 2 arom. H). Anal. calc. for C₄₄H₈₀BrN₃O₄ (795.03): C 66.47, H 10.14, N 5.29; found: C 66.62, H 10.28, N 5.31.

1-[(2S)-6-[Dodecanoyl(amino)]-2-[undecanoyl(amino)]hexanoyloxy]undecyl]pyridinium Bromide (2f). Same procedure as for **2a**, but with **6f**. Yield: 97%. M.p. 87–88°. IR (KBr): 3315, 1720, 1637, 1543. ¹H-NMR (400 MHz, CDCl₃): 0.88–0.90 (*m*, 2 Me); 2.17 (*t*, *J* = 8.1, CH₂CONH); 2.25 (*t*, *J* = 7.3, NHCOCH₂); 3.22 (*q*, *J* = 3.9, NHCH₂); 4.05–4.16 (*m*, OCH₂); 4.49–5.04 (*m*, CHNH); 6.26 (*t*, *J* = 5.6, N^oH); 6.64 (*d*, *J* = 7.6, N^oH); 8.15 (*t*, *J* = 6.8, 2 arom. H); 8.52 (*t*, *J* = 7.6, arom. H); 9.48 (*t*, *J* = 5.3, 2 arom. H). Anal. calc. for C₄₅H₈₂BrN₃O₄ (809.05): C 66.80, H 10.22, N 5.19; found: C 66.99, H 10.45, N 5.22.

1-[(2S)-2,6-Bis[dodecanoyl(amino)]hexanoyloxy]undecyl]pyridinium Bromide (2g). Same procedure as for **2a**, but with **6g**. Yield: 97%. M.p. 88–89°. IR (KBr): 3316, 1720, 1637, 1543. ¹H-NMR (400 MHz, CDCl₃): 0.88 (*t*, *J* = 6.6, 2 Me); 2.16–2.26 (*m*, 2 CH₂CONH); 3.23 (*q*, *J* = 6.3, NHCH₂); 4.07–4.15 (*m*, OCH₂); 4.50 (*q*, *J* = 3.3, CHNH); 6.10 (*t*, *J* = 6.1, N^oH); 6.45 (*d*, *J* = 7.6, N^oH); 8.13 (*t*, *J* = 6.8, 2 arom. H); 8.50 (*t*, *J* = 7.6, arom. H); 9.52 (*t*, *J* = 5.6, 2 arom. H). Anal. calc. for C₄₆H₈₄BrN₃O₄ (823.08): C 67.12, H 10.29, N 5.11; found: C 67.23, H 10.41, N 5.15.

3-[(2S)-6-[Dodecanoyl(amino)]-2-[hexanoyl(amino)]hexanoyloxy]undecyl]-1-methyl-1H-imidazolium Bromide (3). A DMF soln. (20 ml) of **6a** (10 mmol) and 1-methyl-1H-imidazole (100 mmol) was heated at 100° for 48 h under N₂. Et₂O (150 ml) was added, and the soln. was allowed to stand in a refrigerator for 6 h. The white precipitate was filtered, washed with Et₂O, and dried. The crude product was recrystallized twice from AcOEt/Et₂O to afford 92% of **3**. M.p. 78–80°. IR (KBr): 3306, 1735, 1639, 1542. ¹H-NMR (400 MHz, CDCl₃): 0.88 (*m*, 2 Me); 2.17 (*t*, *J* = 8.1, CH₂CONH); 2.25 (*t*, *J* = 7.3, NHCOCH₂); 3.22 (*q*, *J* = 6.3, NHCH₂); 4.12 (*s*, Me–C(1)); 4.32 (*t*, *J* = 7.3, OCH₂); 4.46–4.51 (*m*, CHNH); 6.33 (*t*, *J* = 5.5, N^oH); 6.62 (*d*, *J* = 7.6, N^oH); 7.43 (*t*, *J* = 1.7, Hz, H–C(4)); 7.51 (*t*, *J* = 1.5, H–C(5)); 10.28 (*s*, H–C(2)). Anal. calc. for C₃₉H₇₃BrN₄O₄ (741.93): C 63.14, H 9.92, N 7.55; found: C 63.44, H 10.18, N 7.64.

REFERENCES

- [1] P. Terech, R. G. Weiss, *Chem. Rev.* **1997**, *97*, 3133; P. Terech, *Ber. Bunsenges. Phys. Chem.* **1998**, *102*, 1630; J. H. van Esch, B. L. Feringa, *Angew. Chem., Int. Ed.* **2000**, *39*, 2263; D. J. Abdallah, R. G. Weiss, *Adv. Mater.* **2000**, *12*, 1237.
- [2] K. Hanabusa, H. Nakayama, M. Kimura, H. Shirai, *Chem. Lett.* **2000**, 1070; J. H. van Esch, B. L. Feringa, *Angew. Chem., Int. Ed.* **2000**, *39*, 2263; M. de Loos, J. van Esch, R. M. Kellogg, B. L. Feringa, *Angew. Chem., Int. Ed.* **2001**, *40*, 613; G. Mieden-Gundert, L. Klein, M. Fischer, F. Vögtle, K. Heuzé, J.-L. Pozzo, M. Vallier, F. Fages, *Angew. Chem., Int. Ed.* **2001**, *40*, 3164; H. M. Willemen, T. Vermonden, A. T. M. Marcelis, E. J. R. Sudhölter, *Eur. J. Org. Chem.* **2001**, 2329; K. S. Partridge, D. K. Smith, G. M. Dykes, P. T. McGrail, *Chem. Commun.* **2001**, 319; R. P. Lyon, W. M. Atkins, *J. Am. Chem. Soc.* **2001**, *123*, 4408; A. Ajayaghosh, S. J. George, *J. Am. Chem. Soc.* **2001**, *123*, 5148; U. Beginn, B. Tartsch, *Chem. Commun.* **2001**, 1924; A. Friggeri, O. Gronwald, K. J. C. van Bommel, S. Shinkai, D. N. Reinhoudt, *J. Am. Chem. Soc.* **2002**, *124*, 10754.
- [3] W. Gu, L. Lu, G. B. Chapman, R. G. Weiss, *Chem. Commun.* **1997**, 543; R. J. H. Hafkamp, B. P. A. Kokke, I. M. Danke, H. P. M. Geurts, A. E. Rowan, M. C. Feiters, R. J. M. Nolte, *Chem. Commun.* **1997**, 545; S. Kobayashi, K. Hanabusa, N. Hamasaki, M. Kimura, H. Shirai, S. Shinkai, *Chem. Mater.* **2000**, *12*, 1523; J. H. Jung, H. Kobayashi, M. Masuda, T. Shimizu, S. Shinkai, *J. Am. Chem. Soc.* **2001**, *123*, 8785; S. Kobayashi, N. Hamasaki, M. Suzuki, M. Kimura, H. Shirai, K. Hanabusa, *J. Am. Chem. Soc.* **2002**, *124*, 6550.
- [4] S. Li, V. T. John, G. C. Irvin, S. H. Bachakonda, G. L. McPherson, C. J. O'Connor, *J. Appl. Phys.* **1999**, *85*, 5965; N. Velasco-Garcia, M. J. Valencia-González, M. E. Diaz-Garcia, *Analyst* **1997**, *122*, 5008.
- [5] K. Hanabusa, K. Hiratsuka, M. Kimura, H. Shirai, *Chem. Mater.* **1999**, *11*, 649; N. Mizoshita, K. Kutsuna, K. Hanabusa, T. Kato, *J. Photopolym. Sci. Technol.* **2000**, *13*, 307; L. Gu, Y. Zhao, *Chem. Mater.* **2000**, *12*, 3667; F. Placin, J.-P. Desvergne, J.-C. Lasségus, *Chem. Mater.* **2001**, *13*, 117; W. Kubo, K. Murakoshi, T. Kitamura, S. Yoshida, K. Hanabusa, H. Shirai, Y. Wada, S. Yanagida, *J. Phys. Chem. B* **2001**, *105*, 12809; W. Kubo, T. Kitamura, K. Hanabusa, Y. S. Yanagida, *Chem. Commun.* **2002**, 374.
- [6] N. A. Peppas, Y. Huang, M. Tottes-Lugo, J. H. Ward, J. Zhang, *Annu. Rev. Biomed. Eng.* **2000**, *2*, 9; R. Langer, *Acc. Chem. Res.* **2000**, *33*, 94; K. Yong, D. J. Mooney, *Chem. Rev.* **2001**, *101*, 1869.
- [7] B. Zhao, J. S. Moore, *Langmuir* **2001**, *17*, 4758; Y. Luo, P. D. Dalton, M. S. Shoichet, *Chem. Mater.* **2001**, *13*, 4087; V. Pardo-Yissar, R. Gabai, A. N. Shipway, T. Bourenko, I. Willner, *Adv. Mater.* **2001**, *13*, 1320; Z. Hu, X. Lu, J. Gao, *Adv. Mater.* **2001**, *13*, 1708.

- [8] J.-H. Fuhrhop, W. Helfrich, *Chem. Rev.* **1993**, 93, 1565; S. Bhattacharya, S. N. G. Acharya, *Chem. Mater.* **1999**, 11, 3504; L. A. Estroff, A. D. Hamilton, *Angew. Chem., Int. Ed.* **2001**, 39, 3447; S. Bhattacharya, S. N. G. Acharya, *Langmuir* **2000**, 16, 87; F. M. Menger, K. L. Caran, *J. Am. Chem. Soc.* **2000**, 122, 11679; U. Maitra, S. Mukhopadhyay, A. Sarkar, P. Rao, S. S. Indi, *Angew. Chem., Int. Ed.* **2001**, 40, 2281; M. Amaike, H. Kobayashi, S. Shinkai, *Chem. Lett.* **2001**, 620; J.-H. Jung, G. John, M. Masuda, K. Yoshida, S. Shinkai, T. Shimizu, *Langmuir* **2001**, 17, 7229; J. Makarević, M. Kokić, B. Perić, V. Tomišić, B. Kojić-Prodić, M. Žinić, *Chem.–Eur. J.* **2001**, 7, 3328; B. A. Simmons, G. C. Irvin, V. Agarwal, A. Rose, V. T. John, G. L. McPherson, N. P. Balsara, *Langmuir* **2002**, 18, 624; M. Suzuki, M. Yumoto, M. Kimura, H. Shirai, K. Hanabusa, *New J. Chem.* **2002**, 26, 817.
- [9] M. Suzuki, M. Yumoto, M. Kimura, H. Shirai, K. Hanabusa, *Chem. Commun.* **2002**, 884; M. Suzuki, M. Yumoto, M. Kimura, H. Shirai, K. Hanabusa, *Chem.–Eur. J.* **2003**, 9, 348.
- [10] N. Yamada, T. Imai, E. Koyama, *Langmuir* **2001**, 17, 961; X. Wang, Y. Shen, Y. Pan, Y. Liang, *Langmuir* **2001**, 17, 3162.
- [11] F. H. Billiot, M. McCarroll, E. J. Billiot, J. K. Rugutt, K. Morris, I. M. Warner, *Langmuir* **2002**, 18, 2993.

Received February 7, 2003